OPTIMIZATION OF SUPPORTS IN METAL-BASED ADDITIVE MANUFACTURING BY MEANS OF FINITE ELEMENT MODELS

T. A. Krol[a], M. F. Zaeh[b] and C. Seidel[a]

[a] *iwb* Application Center Augsburg, Technische Universitaet Muenchen,
Beim Glaspalast 5, 86153 Augsburg, Germany
[b] Institute for Machine Tools and Industrial Management (*iwb*), Technische Universitaet Muenchen,
Boltzmannstr. 15, 85748 Garching, Germany

Abstract

Metal-based additive manufacturing processes require a supporting of overhanging part areas during the powder solidification e. g. for improving the heat dissipation to the substrate. Technology users nowadays strive to reduce support areas due to economical aspects, while simultaneously enhancing the process stability by maximizing the support stiffness. For the simplification and acceleration of this support design procedure, the presented work describes a methodology for optimizing support structures by means of finite element models. Thereby, the main approaches are covering a fractal adaptation of the support layout and an optimization of block supports depending on the calculation results. The presented methods were applied by using experimental components.

Introduction

Additive manufacturing processes are increasingly used for the industrial production of complex and highly individualized parts (cf. ZAEH 2006, GEBHARDT 2007). Nowadays, different market segments are addressed due to the named advantages (e. g. dental and automotive industry, tool- and mold-making). In particular, metal- and powder-based layered technologies are enabling a production of functional parts in a single work step. By utilizing these technologies for the manufacturing of prototypes, performing functional tests of industrial components directly at the place of action becomes possible. However, in contrary to plastic processes, higher temperature gradients are present due to the melting of metal alloy powders (e. g. AlSi12). These can be compared to the ones which are present in similar thermally influenced processes (for example laser welding). The acting gradient causes thermal strains and stresses which are described by the "Temperature-Gradient-Mechanism" (cf. BRANNER 2010) and can lead to a part depending production failure. A decrease in the resulting part quality can be the consequence. Fig. 1 shows technology specific process failures for different manufacturing examples.

part distortions due to temperature gradients

support delamination during manufacturing

Fig. 1: Process failures of metal- and powder-based additive manufacturing

The shaping of the visualized part distortions (cf. Fig. 1) is dependent on the used process parameters (e. g. laser power and velocity, scan pattern). A production without manufacturing errors (due to deformations) therefore

requires high process knowledge to correctly adjust defined part-, process- and material-specific parameter values. As VAN ELSEN (2007) described in his work, these conditions cannot always be reached due to the process complexity.

Fig. 1 shows that support structures for product manufacturing by means of metal- and powder-based additive processes are used (cf. VAN ELSEN 2007, KROL ET AL. 2011B). These structures are exhibiting firstly the function for heat dissipation from overhanging part areas to the substrate (building plate) and are secondly protecting these part sections from displacing during manufacturing. After the process is finished, these additional support structures are separated from the part and are then disposed. Hence, these constructions are not creating value. Therefore, a filigree support design is often used to save material resources. For designing the support structure the consideration of thermo-mechanical properties is not always performed. The impacts of residual stresses on the resulting process stability are frequently unknown. Hence, a displacement of the structure during the manufacturing procedure can be the consequence. In worst case, this can lead to a process interruption before the process is finished. This scenario is displayed in Fig. 2.
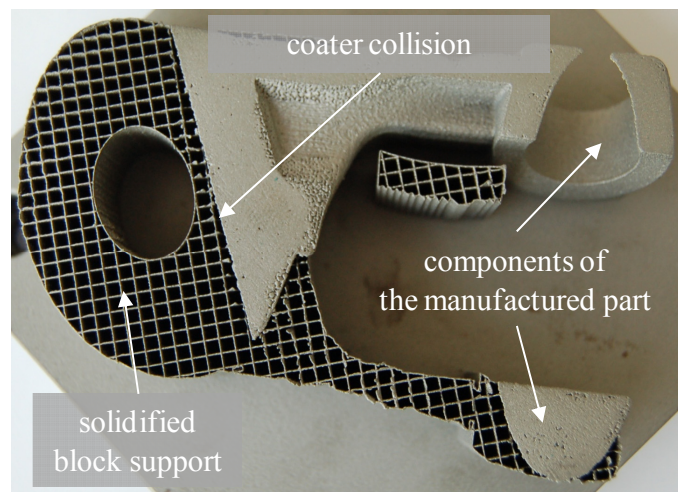

Fig. 2: Process interruption due to distortions in the support area

Within this example of the manufacturing of a robot's wrist the powder coater collides at the part edge between the solidified block shaped support structure and the part layers as a result of layer delamination. A repeated production of the same part, while changing the support design as well as the process parameter constellation, should be performed by the customer to increase the process stability. This iterative procedure leads to high resource consumption and reduces the previously mentioned usability of this technology. Different institutions and scientists are exploring possibilities for an analytical and experimental optimized dimensioning of these structures (cf. ALEXANDER ET AL. 2000, LAN ET AL. 1997). The advantages of the simulation for a virtual process mapping and qualification are investigated by KOLOSSOV (2005) and COSTA ET AL. (2005) in their work. Furthermore, numerical approaches for analyzing metal- and powder-based additive technologies are available within the state of the art (cf. PATIL ET AL. 2007, GUSAROV ET AL. 2010). ZAEH ET AL. (2009) are describing a continuum-mechanical modeling of block supports. These approaches are the basis for the research results presented within this work. The overall objective of the presented methods within this paper is to provide a guideline for a support dimensioning not only with respect to economical aspects, but also under consideration of the calculated thermo-mechanical properties (residual stresses and distortions). This calculation is performed by using the finite element analysis (FEA).

Support Geometries

Different software tools are commercially available for a data preparation and the creation of part-specific support structures. Thereby, the customer can choose between different basic forms of supports. These are displayed in the following Fig. 3 as a brief extraction. While block supports are rather applied for volumetric massive parts (e. g. tool forms), the line support structure is used for manufacturing of complex sheet metal

parts (e. g. components of the automotive industry). In Contrast, point supports are enabling the support of individual part areas.

The user has the possibility to apply different detailing levels and to adjust several parameters based on the described basic geometries for supports. It is for example possible to adapt the design of the connection structure between the support basic geometry and the overhanging lower part surface. This should ease the removal of the supports from the product after the manufacturing process. Furthermore, the grid distance between every single block support wall can be customized for every kind of application.
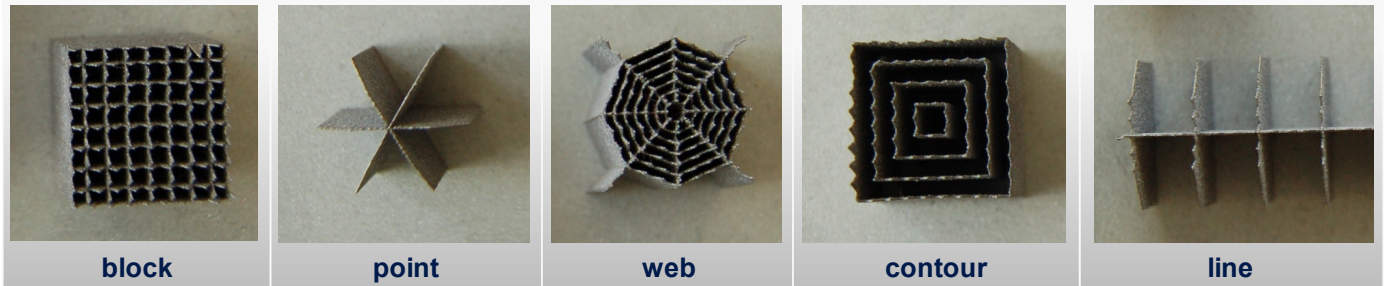

Fig. 3: Different support geometries for metal- and powder-based additive manufacturing

A performed internal survey among technology users, developers and service providers at the *iwb* Application Center Augsburg pointed out that the conventional block and line supports are the most frequently used structures. To get in line with this application trend, the presented methods for optimizing support structures are performed by using block supports.

The manufacturing flexibility and producible geometry variety of additive technologies are enabling the design of specialized support geometries. This feature allows to develop fundamentally new support structures which can be stiffened dependent on the process-related forces. In consideration of these boundary conditions the use of fractal geometries allows to subdivide a basic geometry (e. g. triangles, cf. Fig. 4) into smaller, self-similar geometry shapes (in the displayed case: triangles).
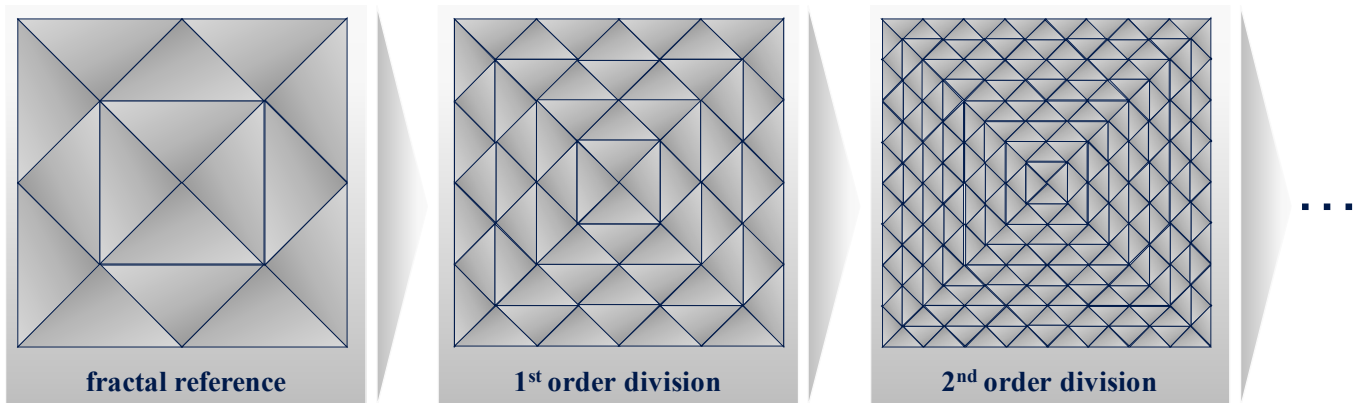

Fig. 4: Top-view of a fractal support structure and stiffening of this structure by means of subdivision

Within the example of Fig. 4 the fractal objects represent right-angled and isosceles triangles. The picture shows top views of the structure (vertically to the building direction). The lines are displaying the support walls, whereas the grey deposited sections are demonstrating the powder areas. For the configuration of the fractal reference geometry it should be taken into account that the distance between the edges of the triangles does not exceed a material-specific value predetermined by the system manufacturer. Based on this reference definition the original triangles can be subdivided in equivalent but smaller triangles. The fractal approach can be continued until the value of the edge length of a triangle is lower than the track width of the laser system (approx. 200 µm). In this case the termination criterion is reached, because the support areas represent a continuous solid material.

Both, the fractal support geometry and the selected block support structure, are enabling a contribution of additional stiffening constructions because of their filigree reference shape. The support adaption is performed by using thermo-mechanical simulation results, whereas the initially mentioned process stability can be increased essentially. Hence, a repeated part manufacturing for a quality enhancement should be prevented with this procedure. Initially, methods for mapping of the mentioned supports within the finite element analysis should be developed and are described in the following.

Numerical Modeling

In the state-of-the-art ZAEH ET AL. (2009) are describing the procedure for mapping of supports with the finite element analysis. As mentioned initially, these approaches are exclusively referring to a continuum-mechanical adaption of block support structures. This method provides a modeling of a solid object for the support area and the possibility of adjusting anisotropic material attenuation factors. However, this alignment of the material parameters of an original filigree structure on a continuum volume exhibits some boundary conditions concerning the calculation accuracy. A usage of irregular or wide meshed block support structures is impossible.

The modeling approaches described by KROL ET AL. (2011B) are based on a high level of detail and are therefore enabling a more accurate mapping of support geometries within the finite element analysis. These modeling types are allowing also the use of solid material models for the support areas described by KROL ET AL. (2011B) (e. g. for AlSi12). The use of empirically determined material factors is not necessary anymore and an increase in the result accuracy is expected. The procedure of transferring the support geometries to the simulation is comparable to the one described by BRANNER (2010). In Fig. 5 this sequence is shown for a cantilever geometry.
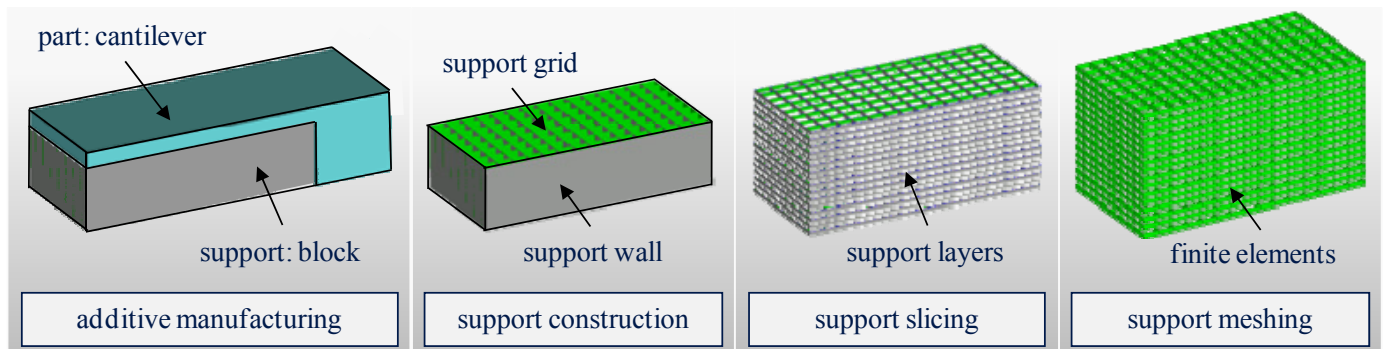

Fig. 5: Transfer of the support geometry from CAD - data to the finite element analysis (FEA)

A support geometry should be designated for the overhanging wing area of the displayed cantilever in Fig. 5. The construction of the support area is performed by transferring the CAD part geometry in a data preparation tool. After slicing the geometry into single layers, the generated data are not transmitted to the manufacturing system, but directly imported into the simulation environment. This procedure is described by KROL ET AL. (2009). With the application of this process chain a numerical interpretation of the support structure and the corresponding part geometry becomes possible.

By using the finite element analysis KROL ET AL. (2011A) are furthermore describing the subdivision of single structural process components into four essential numerical definitions. Within the actual modeling technology, the part geometry is mapped in the simulation by using cubic shaped and directly linked element descriptions. This enables a splitting of elements vertically to the building direction and hence the subdivision into single layers. Thus, a selective and layerwise part building will also become possible within the simulation environment by the use of so called shell elements. For the used cantilever (cf. Fig. 5) the chosen meshing options can be extracted from the following Fig. 6. Hence, element dimensions of 1 x 1 x 0,5 mm³ are used for the part, whereas for the support structure 2½-D descriptions are applied. The specification of an element

thickness can be stored by the user for the support elements. Hence, the strut thickness that is corresponding to the track width of the laser system can also be parameterized virtually.
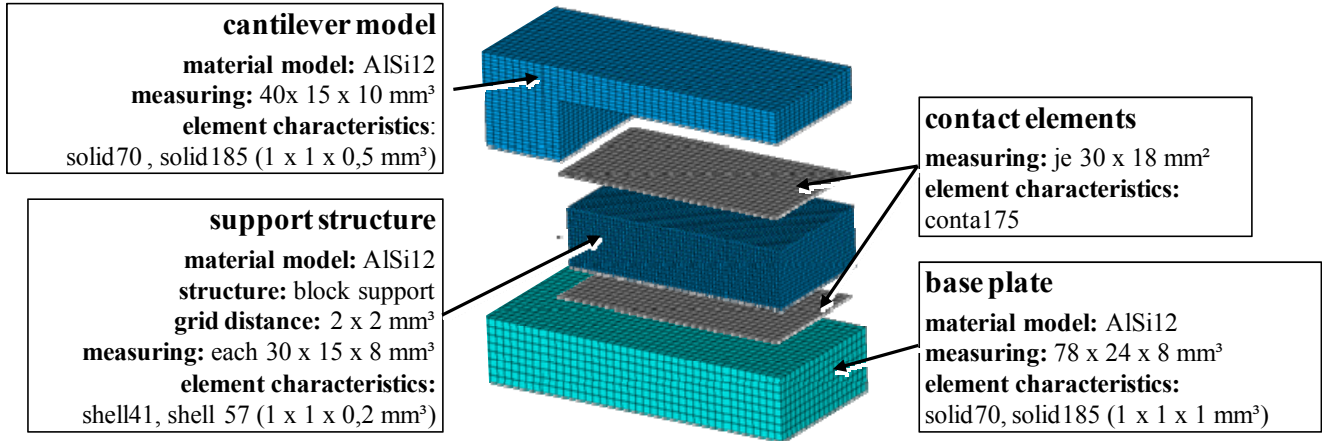

cantilever model
material model: AlSi12
measuring: 40x 15 x 10 mm³
element characteristics:
solid 70 , solid 185 (1 x 1 x 0,5 mm³)

support structure
material model: AlSi12
structure: block support
grid distance: 2 x 2 mm³
measuring: each 30 x 15 x 8 mm³
element characteristics:
shell41, shell 57 (1 x 1 x 0,2 mm³)

contact elements
measuring: je 30 x 18 mm²
element characteristics:
conta175

base plate
material model: AlSi12
measuring: 78 x 24 x 8 mm³
element characteristics:
solid 70, solid 185 (1 x 1 x 1 mm³)

Fig. 6: Numerical components of the cantilever specimen

For the connection of both mesh topologies, the part and support structure are coupled numerically for transferring calculation results between these components. The use of so called contact elements are enabling the transfer of transient and temperature-dependent calculation results from a next higher to a previous layer. KROL ET AL. (2011A) describe that because of the direct joint of support and part area a heat transfer can be modeled exclusively by the following equation (cf. RUST 2009, ANSYS 2007):

$$\frac{\delta Q}{\delta t} = K_C \left(\frac{\delta T_T}{\delta t} - \frac{\delta T_C}{\delta t} \right)$$

Equation 1

Q is defined as the heat flux which is calculated by the thermal equilibrium equation, K_C is the thermal contact conductance coefficient, T_T describes the resulting temperature at the target surface and T_C is defined as the temperature at the contact surface.

Based on this definition the structural distortions are transmitted by the contacts with changing the degrees of freedom to a thermo-mechanical description. This is performed by using the "Augmented Lagrange Method" (RUST 2009). Hence, for closing the contact gapping the pressure is defined in the following equation (ANSYS 2007):

$$P = \begin{cases} 0 & if \ u_n > 0 \\ K_n \times u_n + \lambda_{i+1} & if \ u_n \leq 0 \end{cases}$$

Equation 2

Within this equation K_n is the contact normal stiffness, u_n describes the contact gap size and λ_{i+1} is defined by the following correlation (cf. ANSYS 2007):

$$\lambda_{i+1} = \begin{cases} \lambda_i + K_n \times u_n & if \ |u_n| > \varepsilon \\ \lambda_i & if \ |u_n| < \varepsilon \end{cases}$$

Equation 3

Hence, λ_i describes the Lagrange multiplier component at the iteration i whereas ε is the compatibility tolerance.

Furthermore, it is necessary to model a building plate for the application of thermal boundary conditions (e. g. convection surfaces) and mechanical specifications (e. g. elastic bedding). The named definitions can be applied at the lateral surface and bottom side by using this substrate section. With the construction of the substrate and the other named numerical components, the analysis of different supports in the finite element analysis concerning their influence on residual stresses and distortions becomes possible.

<u>Calculation-Dependent Stiffening of Supports</u>

The definition of an objective function is decisive for the thermo-mechanical optimization of the support structure design. Hence, with using an equation the residual stresses and distortions should be significantly lowered and a risk of an early process interruption during manufacturing should be prevented (cf. Fig. 2). This means that high process-related residual stresses should be minimized within critical areas in the support structure and should be lowered or translocated into the stiffer part sections. Thus, a delamination of supports within the building progress could be prevented.

To characterize the state of residual stresses numerically, the definition of material models for the adaption of the material behavior in the finite element analysis is required. For solving the thermo-mechanical simulation problem the definition of a material matrix is necessary, which is displayed in Equation 4 (ANSYS 2007):

$$[D]^{-1} = \begin{bmatrix} \frac{1}{E_X} & -\frac{v_{XY}}{E_X} & -\frac{v_{XZ}}{E_X} & 0 & 0 & 0 \\ -\frac{v_{YX}}{E_Y} & \frac{1}{E_Y} & -\frac{v_{YZ}}{E_Y} & 0 & 0 & 0 \\ -\frac{v_{ZX}}{E_Z} & -\frac{v_{ZY}}{E_Z} & \frac{1}{E_Z} & 0 & 0 & 0 \\ 0 & 0 & 0 & \frac{1}{G_{XY}} & 0 & 0 \\ 0 & 0 & 0 & 0 & \frac{1}{G_{YZ}} & 0 \\ 0 & 0 & 0 & 0 & 0 & \frac{1}{G_{XZ}} \end{bmatrix} \qquad \text{Equation 4}$$

E_X, E_Y and E_Z are the Young's modulus for the single Cartesian spatial direction. v_{XY}, v_{XZ}, v_{YX}, v_{YZ}, v_{ZX} and v_{ZY} are described as the Poisson's ratios defined by Cartesian planes. Finally, G_{XY}, G_{YZ} and G_{XZ} are representing the shear modules for the corresponding planes.

The stresses parallel to the building direction (Branner 2010) are responsible for the failure mechanisms of supports. In order to define the stresses in z-direction, this Cartesian oriented stress component can be extracted from the stress-strain relation (e. g. multilinear kinematic hardening, cf. KROL ET AL. 2011B) and additionally with the creation of the stiffness matrix. A resolution of the used system of equation provides the following correlation that in this case is also used for the calculation (ANSYS 2007):

$$\sigma_Z = \frac{E_Z}{h} \times (v_{XZ} + v_{YZ} \times v_{XY}) \times (\varepsilon_X - \alpha_X \times \Delta T) + \frac{E_Z}{h} \times \left(v_{YZ} + v_{XZ} \times v_{XY} \times \frac{E_Y}{E_X}\right) \quad \times (\varepsilon_Y - \alpha_Y \times \Delta T) + \frac{E_Z}{h} \times$$
$$\left(1 - v_{XY}{}^2 \times \frac{E_Y}{E_X}\right) \times (\varepsilon_Z - \alpha_Z \times \Delta T) \qquad \text{Equation 5}$$

In addition to equation 4, ε_X, ε_Y and ε_Z are defined as strains in the corresponding Cartesian spatial direction. Furthermore, α_X, α_Y and α_Z are representing the coefficients of thermal expansion and ΔT is the difference in temperature from the actual to the next solving step in the simulation. Finally h is defined by the following equation (ANSYS 2007):

$$h = 1 - v_{XY}{}^2 \times \frac{E_Y}{E_X} - v_{YZ}{}^2 \times \frac{E_Z}{E_Y} - v_{XZ}{}^2 \times \frac{E_Z}{E_X} - 2 \times v_{XY} \times v_{YZ} \times v_{XZ} \times \frac{E_Z}{E_X} \qquad \text{Equation 6}$$

With this definition and the already described simulation models, an improvement concerning the state of residual stresses in the support structure can be reached. As announced before, block support structures should be applied to develop optimization algorithms. Hence, the following Fig. 7 portrays a suitable scenario. On the right upper side a part section with the underlying and corresponding support is illustrated. This structure exhibits a grid distance of 2 x 2 mm² vertically to the building direction, whereas the overall dimensions cover an area of 6 x 6 mm². This structure is 5 mm in height. Single top views of the named support structures are also added in Fig.7. Corresponding to Fig. 4, the black colored lines are the connection lines of the support walls, while the red and green colored sections are displaying the powder material within the process.
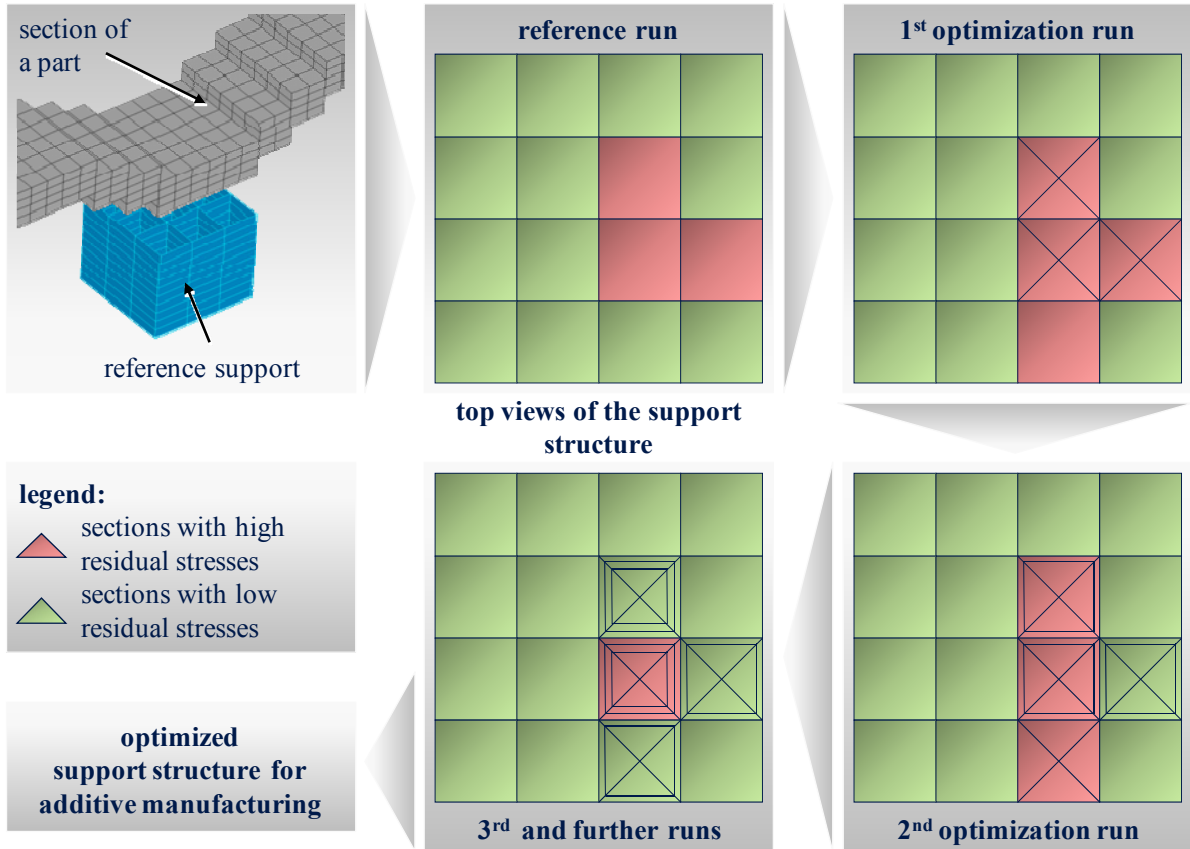
Fig. 7: Functionality of the block support optimization

For the execution of a thermo-mechanical calculation with the presented simulation models residual stresses in building direction can be derived from the corners (nodes) of every single support cell. The selection of suitable nodes within the structure is of essential importance for the optimization. Therefore, the user should choose node locations, in which a high layer delamination risk within the real building process can be assumed. Thereby, an overdeterminacy of the stress status in x- and y-direction can be prevented. Depending on the conditions of compressive and tensile stresses within the nodal selection, an objective function can be defined. For the insertion of stiffening options every single support cell is considered. Based heron, the numerical values of the corresponding stresses at the related nodes are averaged for every single cell. Subsequently, all stress values of the reference run are averaged while using the whole selected nodal set. This value is then compared with the previously calculated variables for every single support cell. If the value of a cell is less than the total value of the whole support structure, a stiffening at this position is not necessary. This case is displayed exemplarily in Fig. 7 by the green highlighted cell sections in the support top view. In the opposite case, an additional stiffening of the support cell is performed, shown in Fig. 7 by the red highlighted cell sections. The described relations within this paragraph can be characterized by the following equation:

$$\frac{1}{n_n} \times \sum_{k=1}^{n_n} \sigma_{Z,k} < a_F \times \frac{1}{n_{(max)}} \times \sum_{i=1}^{n_{(max)}} \sigma_{Z,i} \qquad \text{Equation 7}$$

n_n describes the amount of nodes within one support cell (for block supports: $n_n = 4$), whereas $n_{(max)}$ is the amount of all selected nodes for the support optimization. $\sigma_{Z,k}$ and $\sigma_{Z,i}$ are representing the related stress states in building direction as it is described previously by equation 5. The additionally introduced factor a_F enables a user-dependent specification of stronger criteria for stiffening of support structures (reference: $a_F = 0.8$). When using the reference dimension, the average of all selected node values is lowered. In the reverse case, a value of greater one results in a weaker factor dimensioning. Hence, the customer can adjust the exertion of influence for the proposed methodologies concerning the amount of stiffening sections and therefore the additionally

713

solidified support material. This also enables the consideration of economical aspects for the designing of supports. Therefore, the relationship between the additionally solidified support volume (due to insertion of stiffening sections) is referring to the initial volume of the basic support geometry and is described by the following equation 8:

$$Solid\ Ratio = \frac{A_n}{A_0} \hspace{6cm} \text{Equation 8}$$

Thus, A_0 describes the initial volume of the support structure, while A_n comprises the volume of added stiffening procedures. It should be distinguished between the support stiffening options presented in Fig. 7 to define A_n for block support structures. Whereas the first optimization cycle is providing a diagonal connection to the already existing support walls, the following optimization cycles are including further stiffening rips. A graded procedure should be selected during these cycles. While red colored support cells (cf. Fig. 7), which are already containing diagonal walls, should be added to the next step (e. g. within the 3$^{\text{rd}}$ optimization cycle) by the use of one stiffening rip, the other red cells should be extended firstly by a diagonal stiffening. A universally valid formulation of the described relationship can be extracted from the following equation:

$$A_n = \begin{cases} 2.828 \times f_G \times f_L - 4.828 \times f_L{}^2 & if\ n = 1\ and\ f_G \geq 2.414 \times f_L \\ (4n - 1.172) \times f_G \times f_L - (4n^2 + 1.657n - 0.828) \times f_L^2 - (4n^2 - 4n) \times 0.2 \times f_L \\ \hspace{1.5cm} if\ n \geq 2\ and\ \ f_G \geq (2n + 0.414) \times f_L + (2n - 2) \times 0.2 \end{cases} \hspace{1cm} \text{Equation 9}$$

In this equation f_G describes the grid distance of the used block support structure and f_L represents the support wall thickness, which is dependent on the laser track width. The parameter n comprises the actually used optimization cycle of every considered support cell. Accordingly, it can be recorded that the equations for the analytical description of support stiffening is formulated by using three single descriptions (cf. Equation 9). These formulations are the result of the used geometric subdivision properties for the support optimization. Furthermore, the presented approaches are specific formulations for block support structures. Compared with the previously presented fractal geometries, fundamentally different relations are used, which are presented in the following.

For the description of stiffening options of fractal geometries, the same application example that is used in Fig. 7 is selected for following Fig. 8. Differences between these two scenarios are existent for the shape and arrangement of the used support structures. Based on the whole support area as a reference, the partition of this structure is performed by using single rectangular and isosceles triangles. According to the previously named definition, the initial subdivision should exhibit a maximal edge length of 2 mm for every triangle. Hence, a stable supporting of overhanging part areas can also be reached in the reference experiment. Correspondingly, equation 7 can be used as an objective function for nodal results of every single support cell (triangles in this case). However, at this point n_n has a value of 3.

Because of the regularity of the used subdivisions, the additionally solidified areas are represented by using two different descriptions within the following equation:

$$A_{n,max} = \begin{cases} 2.828 \times f_G \times f_L - 4.828 \times f_L{}^2 & if\ n = 1\ and\ f_G \geq 2.414\ \times\ f_L \\ (2.414 \times 2^n - 2) \times f_G \times f_L - (1.457 \times 4^n - 1) \times f_L^2 \\ \hspace{2cm} n \geq 2\ and\ \ f_G \geq 1.207 \times 2^n \times f_L \end{cases} \hspace{1cm} \text{Equation 10}$$

The first equation describes the partition of the reference support into single, fractal triangles, while the lower correlation in equation 10 is valid for further optimization cycles in the used fractal support cells.
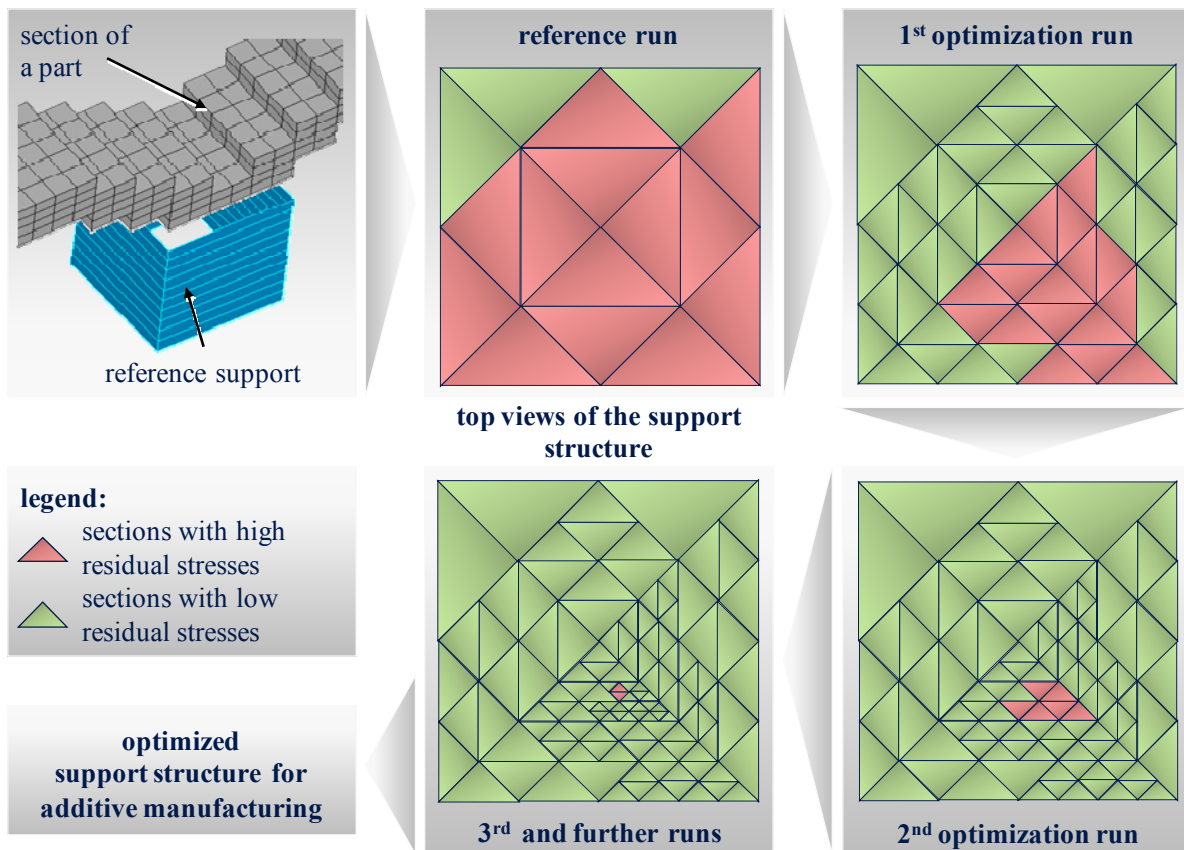
Fig. 8: Functionality for optimizing fractal support geometries

Application of the Methodologies

In the following section the discussed methodologies are applied for a tilde geometry (cf. Fig. 9) by the use of the methodology presented in Fig. 7. Initially, this is performed by using block support structures. From the evaluation of previously executed experimental studies it can be summarized that by using this geometry higher distortion values can be expected compared to the initially shown cantilever form (cf. Fig. 6). This property is of essential meaning for the comparison of simulation results with experimental values. In doing so, the measuring results are not in the range of the measuring equipment accuracy.

According to the definition of Fig. 6 the following Fig. 9 shows the numerical interpretation of the part and support sections as well as the contact definitions.
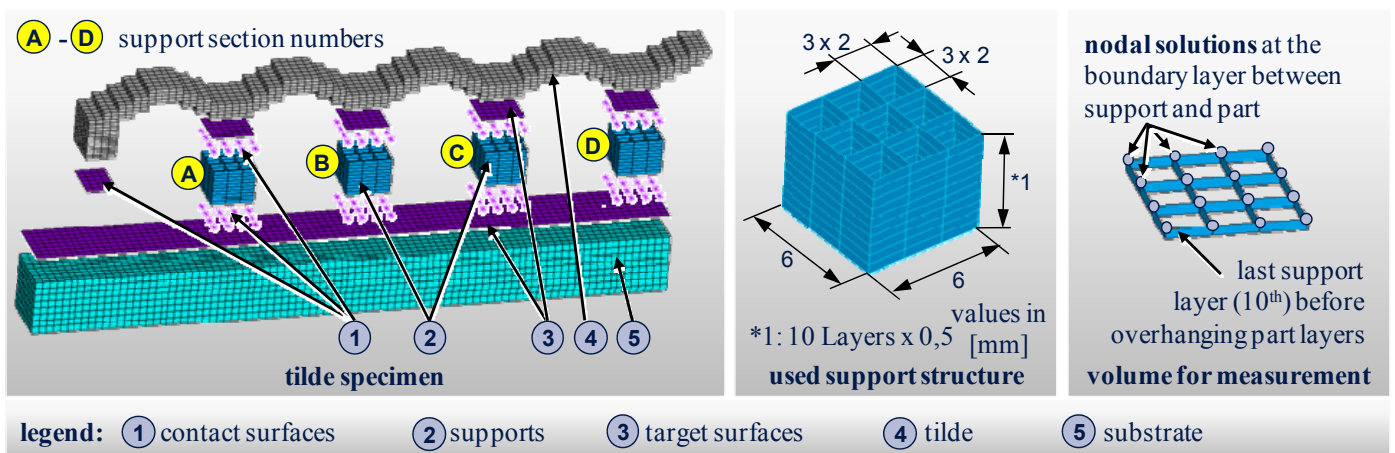

Fig. 9: Test specimen for the application of the support optimization

Four support sections containing block support structures were investigated in this study and are indexed by A, B, C and D. For this configuration support failures are expected at the border areas between the used block structure and the tilde part areas. This led to the selection and subsequently optimization of the corresponding nodes at these positions (cf. also Fig. 9).

The solving of the simulation problem was initially performed with using a conventional block reference geometry as it is visualized in Fig. 9. A listing of the gained results can be extracted from the following Fig. 10. The residual stresses in building direction of the four support sections A to D (cf. Fig 9) are displayed. Beneath the numerical results, the used support structure is displayed in a top view sketch within Fig. 10.
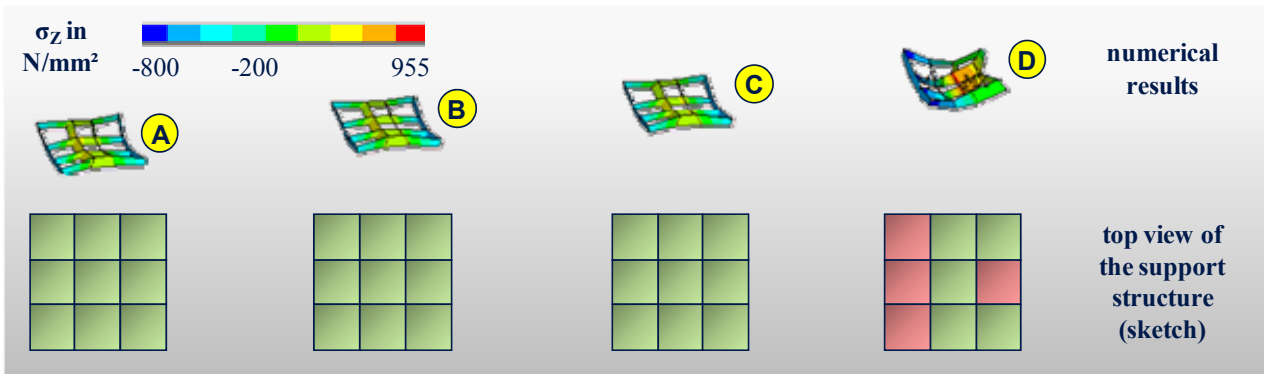

Fig. 10: Reference run for the optimization of block supports

The result of the calculation indicate that tensile and compressive stresses are existent in the selected support sections. The former stresses are responsible for support failures. The corresponding values exhibit a maximum of 955 N/mm² which is clearly above the yield strength of the modeled aluminium alloy (cf. KROL ET AL. 2011B). Accordingly, a high tendency for support failures exists for the red sections displayed in Fig. 10. Hence, a support stiffening should be performed in these sections.

Corresponding to the procedure plan visualized in Fig. 7, the next simulation run should be performed by using an adapted support design. The results are displayed in the following Fig. 11. Due to the shifting of stresses by means of the optimization function, the average value of tensile stresses is lowered for the whole selected support area by 33 % compared to the reference calculation. The additionally solidified material within the support structure (because of the stiffening) exhibits a value of 11 %. The average change should be compared once again and also for every following optimization cycle with the specific values of every support cell (cf. equation 7).
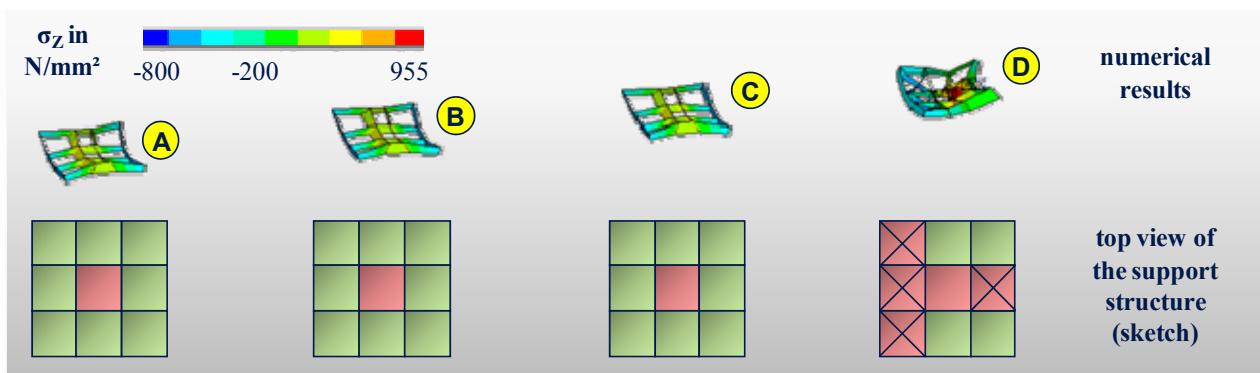

Fig. 11: 1ˢᵗ optimization run

By considering the results of Fig. 11 it becomes evident that by lowering the average value of residual stresses for the selected sections also other support cells should be optimized by using stiffening options. These should be included in the next calculation run. The following Fig. 12 shows the corresponding result of this procedure. For this optimization cycle the average value of tensile stresses for the whole selected support area can again be

lowered by 51 % compared to the reference experiment (cf. Fig 10). This is linked to an increase in solidified material by 36 % towards the original block support structure.
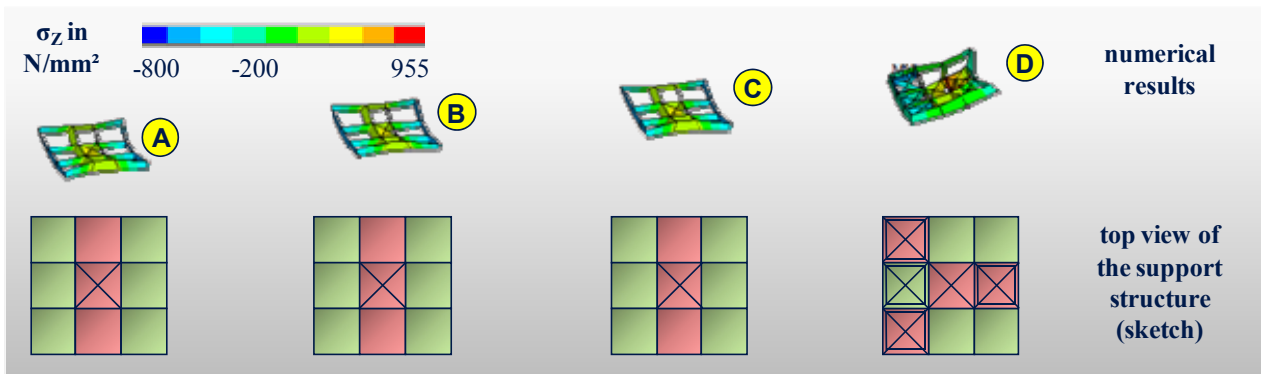

Fig. 12: 2nd optimization run

A subsequently performed optimization cycle is exhibiting further simulation results, whereby, compared to the reference experiment, a lowering of the named average value by 72 % is possible. However, this means an increase in additionally solidified support volume of 72 %. Within this cycle, the stress value for every single support cell is beneath the yield strength of the aluminum alloy, whereas the risk of a delamination of the selected support layer is significantly reduced. An additional optimization step by applying the described methods demonstrates, that an overall stress reduction of 78 % can be reached by having an increase in material consumption of 100 % compared to the reference experiment. At this point the user is asked for transmitting the desired, calculated support adaption cycle. Therefore, the corresponding decision path for the operator is dependent on the desired residual stress state from the actual to the previous optimization run while increasing the additionally solidified support material consumption at the same time. Either this can be the termination criterion for the optimization, or the cycles are performed as long as an asymptotic end value will be achieved (e. g. if defining a volumetric dense and solid support area).

Summary and Future Perspectives

The contents of the presented work are investigated within the research project PartSUPPORT which is founded by the Bavarian Research Foundation. By using the described approaches, a transmitting and lowering of residual stresses in support sections which tend to exhibit failures in the manufacturing process can be achieved. Furthermore, the customer can choose between different simulation models for the adaption and analysis of different support and part geometries. The functionality of the methods for the adaption of support structures depending on the numerical calculated, thermo-mechanical results is exemplary shown by using block supports. Prospectively, the simulation results should be compared with experimental values. With already performed neutron diffractometry measurements at the STRESS-SPEC Instrument of the FRMII in Garching near Munich (Germany), a comparison of the residual stress states is possible and the results will be presented in the near future.

Sources

ALEXANDER ET AL. 2000
Alexander, P.; Dutta, D.: Layered manufacturing of surfaces with open contours using localized wall thickening. Computer-Aided Design 32 (2000), p. 175–189.

ANSYS 2007
ANSYS, Inc.: Release 11.0 Documentation for ANSYS - Heat Flow Fundamentals. 2007.

BRANNER 2010
Branner, G.: Modellierung transienter Effekte in der Struktursimulation von Schichtbauverfahren. Ph.D. thesis. Munich, Germany: Herbert Utz 2010. ISBN: 978-3831640713.

COSTA ET AL. 2005
Costa, L.; Vilar, R.; Reti, T.; Deus, A. M.: Rapid tooling by laser powder deposition: Process simulation using finite element analysis. Acta Materialia 53 (2005) 14, p. 3987-3999.

PATIL ET AL. 2007
Patil, R. B.; Yadava, V.: Finite element analysis of temperature distribution in single metallic powder layer during metal laser sintering. International Journal of Machine Tools & Manufacture 47 (2007) 7-8, p. 1069-1080.

GEBHARDT 2007
Gebhardt, A.: Generative Fertigungsverfahren. Rapid Prototyping, Rapid Tooling, Rapid Manufacturing. 3rd edition. Munich, Germany: Hanser 2007. ISBN: 9783446226661.

GUSAROV ET AL. 2010
Gusarov, A. V.; Smurov, I.: Modeling the interaction of laser radiation with powder bed at selective laser melting. Physics Procedia 5 (2010) Part B, p. 381-394.

KOLOSSOV 2005
Kolossov, S.: Non-Linear Model and Finite Element Simulation of the Selective Laser Sintering Process. Ph.D. Thesis. Institut de production et robotique, ÉCOLE POLYTECHNIQUE FÉDÉRALE DE LAUSANNE. 2005.

KROL ET AL. 2009
Krol, T. A.; Branner, G.; Schilp, J.: Modelle zur thermomechanischen Simulation metallverarbeitender Strahlschmelzprozesse. Proceedings of the ANSYS Conference & 27th CADFEM Users' Meeting 2009. Leipzig, Germany. 19. November 2009.

KROL ET AL. 2011A
Krol, T. A.; Westhaeuser, S.; Zaeh, M. F.; Schilp, J.: Development of a Simulation-Based Process Chain - Strategy for Different Levels of Detail for the Preprocessing Definitions. In: Boedi, R.; Maurer, W. (ed.): ASIM 2011 - 21. Symposium Simulationstechnik. Winterthur, Switzerland. 7.-9. September 2011. ISBN: 978-3-89967-733-1.

KROL ET AL. 2011B
Krol, T. A.; Zaeh, M. F.; Seidel, C.; Schilp, J.: Computational-Efficient Design of Support Structures and Material Modeling for Metal-Based Additive Manufacturing. Proceedings of the ANSYS Conference & 29th CADFEM Users' Meeting 2011. Stuttgart, Germany. 20. October 2011.

LAN ET AL. 1997
Lan, P. T.; Chou, S. Y.; Chen, L. L.; Gemmill, D.: Determining fabrication orientations for rapid prototyping with stereolithography apparatus. Computer-Aided Design 29 (1997) 1, p. 53–62.

RUST 2009
Rust, W.: Nichtlineare Finite-Elemente-Berechnungen. Wiesbaden, Germany: GWV 2009. ISBN: 978-3-8351-0232-3.

VAN ELSEN 2007
van Elsen, M.: Complexity of selective laser melting. Ph.D. Thesis. Katholieke Universiteit Leuven 2007.

ZAEH 2006
Zaeh, M. F.: Wirtschaftliche Fertigung mit Rapid-Technologien. Anwender-Leitfaden zur Auswahl geeigneter Verfahren. *iwb* Application Center Augsburg, Technische Universitaet Muenchen. Munich, Germany: Hanser 2006. ISBN: 9783446228542.

ZAEH ET AL. 2009
Zaeh, M. F.; Branner, G.; Krol. T. A.: A three dimensional FE-model for the investigation of transient physical effects in Selective Laser Melting. Leiria, Portugal. 2009.